ADVNACED MULTI-FUNCTION INGAAS DETECTORS FOR SWIR

O. Ofer [(1)], R. Elishkov [(1)], R. Friedman[(1)], G. Reches[(1)], I. Hirsch[(1)], L. Langoff[(1)], M. Nitzani[(1)], Y. Reem[(1)], C. Jakobson[(1)], I. Pivnik[(1)], E. Louzon[(1)], A. Aharon[(1)], A. Giladi[(1)], R. Fraenkel[(1)] and I. Shtrichman [(1)]

[(1)] SemiConductor Devices, P.O.Box 2250 Haifa 31021, Israel, Email:oreno@scd.co.il

KEYWORDS: SWIR, Infrared detector, InGaAs, multi-function ROIC, LLL, ALPD

ABSTRACT:

The demand for 2D Focal Plane Arrays (FPA) for Short-Wave Infrared (SWIR) imaging has grown significantly over the past decade, due to growing necessities in numerous commercial and defence applications. SWIR imaging using InGaAs technology is ideal for producing high sensitivity and high resolution reflective image for a wide range of light levels from daylight to starlight, and has the advantage of high transmission in problematic atmospheric conditions such as haze, fog and dust. Advanced functions implemented in the Readout Integrated Circuit (ROIC) can increase the effectiveness of the sensor and reduce the Size, Weight and Power (SWaP) of the SWIR camera and system. In this work we present SCD's multi-mode SWIR sensors with 15 and 10 μm pitch with on-die advanced detection and imaging capabilities such as Asynchronous Laser Pulse Detection (ALPD), active and gated imaging, Low Light Level (LLL) imaging, and High Dynamic Range (HDR).

1. INTRODUCTION

Traditionally, Infrared (IR) imaging is driven by night-vision applications. Passive IR cameras, which sense the mid- and long- wavelengths of the IR spectrum (MWIR and LWIR, respectively), rely on thermal radiation without the need for illumination by natural or artificial light sources. However, high-end thermal imaging requires power-hungry cryogenic coolers, which deem them inappropriate for many hand-held and power limited applications. In contrast, short-wave infrared (SWIR) cameras normally require only moderate cooling and temperature stabilization. Furthermore, the image in SWIR is reflective in nature, thus more intuitive and with higher contrast compared to MWIR and LWIR. Consequently, SWIR imaging provides object identification capability that thermal images cannot match. While SWIR imaging at daytime is very effective due to the sun illumination, at dark night the photon flux in the SWIR band is low and imaging is limited. However, even at moon-less night (Low Light Level imaging), natural Night-glow can achieve acceptable Signal to Noise Ratio (SNR) to enable passive SWIR imaging of 10s to 100s of meter ahead. Alternatively, Active or Gated Imaging, namely illuminating the scene by a laser pulse and synchronously opening a fast integration window at a precise timing, enables imaging of targets kms ahead [1].

The Night-glow phenomenon is caused by various chemi-luminescence processes above the mesosphere yielding irradiance of $10^{-9}\div10^{-8}$ W/cm^2/μm across the SWIR band [2]. For low F# imaging, such irradiance induces photocurrent of ~20nA/cm^2 in high Quantum Efficiency (QE) InGaAs detector. Thus, Low Light Level (LLL) passive SWIR imaging requires low dark current density of less than few nA/cm^2 and very low readout noise from the Readout Integrated Circuit (ROIC). Combining the highly sensitive InGaAs Focal Plane array (FPA) with Gated imaging function in the ROIC enables improved imaging for long-range surveillance even at dark nights.

Over the past decade, SCD has developed InGaAs technology and various sensors for SWIR imaging. The InGaAs/InP photodiode array enables high-performance detector, with low dark-current, high QE, broadband (VIS-SWIR) spectral response, and excellent array uniformity and operability. The cut-off wavelength of 1.7μm covers most of the Night-glow spectrum as well as Eye-safe laser wavelengths providing ideal sensing material for passive and active (or gated) LLL imaging.

The *Cardinal* family of SWIR sensors consists of various ROICs flip-chip bonded to InGaAs photodiode arrays, and integrated to Metallic or Ceramic packages, with or without Thermo-Electric Cooler (TEC) [3-5]. The *Cardinal-640* and the *Cardinal-640-LN* incorporate 640×512 (VGA) FPAs with 15μm pitch, and the *Cardinal-1280* is based on 1280×1024 (SXGA) FPA with 10μm pitch. Stabilizing the FPA temperature by TEC normally consumes very low power, which is ideal for battery-operated system. Moreover, TEC-less operation at a normal night (temperature below 30°C) or at daytime (very high photo-current) is possible without compromising performance.

The *Cardinal* family of sensors include Standard and Low-noise Imaging (SIM and LNIM modes), which are discussed in section 2 of the manuscript. Section 3 details the Active and Gated Imaging modes of operation in *Cardinal-640-LN* and *Cardinal-1280*. In Section 4, we review the three generations of Laser Pulse Detection (LPD) mode, which are implemented in the *Cardinal-640* and *Cardinal-1280* sensors, and in the new *SWIFT* Event-based SWIR vision sensor, which incorporate a 640×512 (VGA) InGaAs FPA with 10μm pitch.

2. PASSIVE IMAGING

Unlike MWIR and LWIR thermal imaging, SWIR imaging is due to reflective rather than emissive radiation, which result in a more natural crisp image. Figure *1*: Tower of David and Jerusalem old city wall imaged at night by Cardinal-1280 sensor and F/7 opticsFigure 1 demonstrates passive night SWIR imaging with the *Cardinal-1280* sensor from a distance of 2km with an f/7 lens. In this case, only 1-pt (Offset) Non-Uniformity Correction (NUC) was applied to the raw image. The observed details of the Jerusalem Wall and the Tower of David are remarkable, although the night imaging was prone to city light pollution and to high humidity (>70% RH).

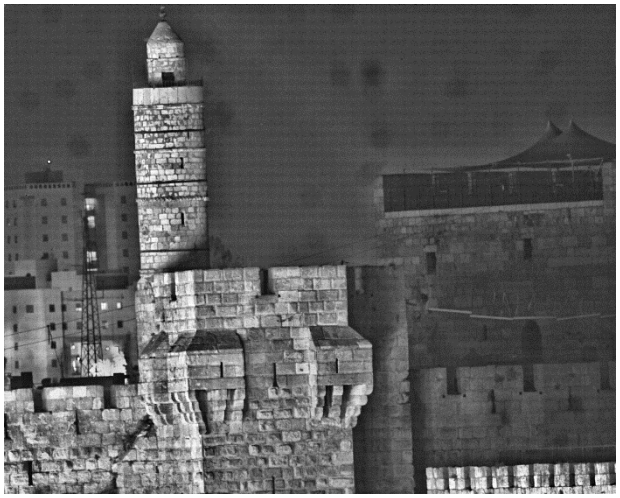

Figure 1: Tower of David and Jerusalem old city wall imaged at night by *Cardinal-1280* sensor and F/7 optics

Yet, the challenges for SWIR imaging are at LLL conditions. Figure *2* shows an image taken inside a forest during a moon-less night with the *Cardinal-640-LN* sensor and F/1.2 optics. The bar target was placed at a distance of approximately 100m from the camera. In this case the FPA temperature was stabilized to 10°C to minimize the dark current. We applied standard 2-point NUC (Gain and Offset) to the raw image.

Figure 2: Bar target imaged by the *Cardinal-640-LN* sensor and F/1.2 optics at Low Light Level conditions

In order to achieve high SNR at LLL conditions, the FPA sensitivity must outperform the low light shot-noise. The most dominant noise contributions from a digital FPA sensor are the dark current shot-noise and the ROIC readout noise. Figure 3 shows the spectral irradiance in SWIR at moon-less night, where the largest radiance contribution is from the Night-glow at 1.4 - 1.65µm, which is spectrally integrated to a typical value of 40nW/cm^2 all year-round [2]. Thermal emission contribution from the 300K background is only substantial above 2µm.

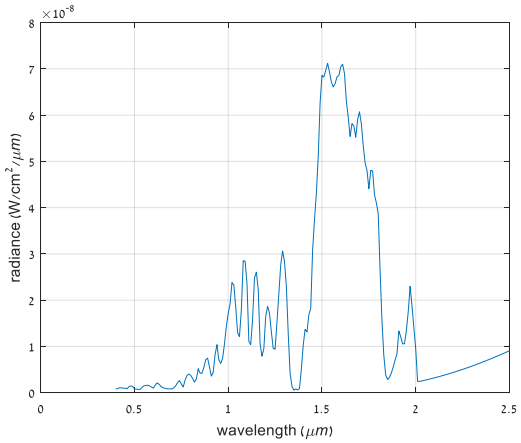

Figure 3: Night-glow and thermal (300K) radiance at SWIR wavelengths on the sensor at f/1

Figure 4 presents the calculated SNR of the *Cardinal* sensors at both High and Low ROIC gains with an f/1.2 lens. For Night-glow only (40nW/cm^2) we find SNR of 10 with the *Cardinal-640-LN* sensor at High gain, which enables decent imaging at moon-less night. A key figure in SWIR imaging is the Noise Equivalent Power (NEP), which is a measure for the required photon power to achieve SNR of 1. As such, it is of particular interest for LLL imaging and is used to define the sensitivity of the detector. The measured NEP of the *Cardinal-640-LN* FPA is presented in Figure 5, and shows mean value of 0.16fW and uniform distribution across the array. Similar behaviour is obtained for the *Cardinal-1280* and *Cardinal-640*.

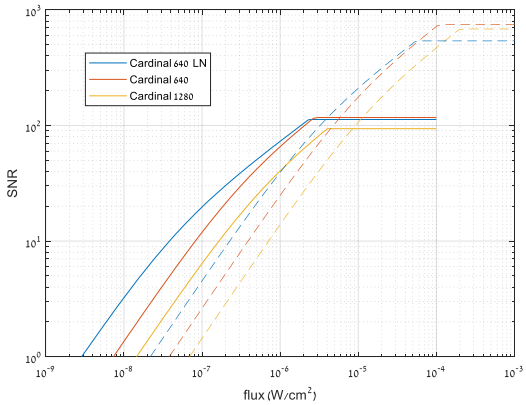

Figure 4: SNR of the *Cardinal* InGaAs sensors versus the integrated SWIR flux at the sensor. The solid (dash) lines represent high (low) gain ROIC integration modes

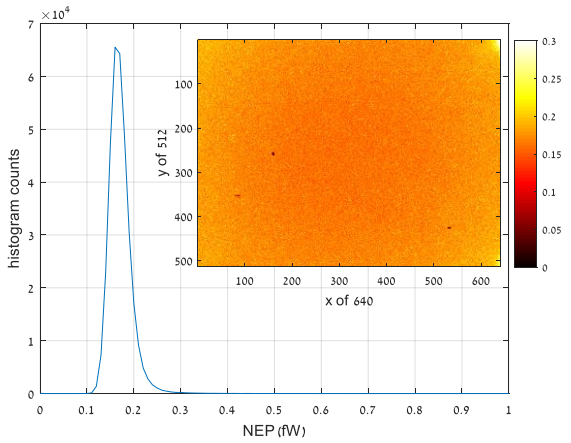

Figure 5: Measured Noise Equivalent Power pixel distribution across *Cardinal-640-LN* FPA at f/2.5. The main panel shows the histogram of the NEP map presented in the inset

3. ACTIVE / GATED IMAGING

Active or Gated Imaging (GI) is a subset of Time-of-Flight (TOF) imaging where a camera with a tightly controlled shutter is used in conjunction with a short pulsed light source. The image contrast and SNR are enhanced by limiting the exposure time of the camera to the return time of the reflected light pulse from an object at a distance *d*. If the light source and camera are collocated, the exposure time should occur at a time *t=2d/c* after the light pulse emission, where *c* is the speed of light. By doing so, only the reflected photons from the object are integrated, while clutter and path reflections in the field of view do not contribute either signal or noise.

The *Cardinal* detectors include a Capacitive Trans-Impedance Amplifier (CTIA) readout circuitry enabling high sensitivity and linearity for the High Gain / Low-Noise Imaging Mode (LNIM) [6]. The CTIA stage enables the use of a relatively small capacitor in the ROIC pixel to obtain low-noise and high sensitivity signal integration, and also provides stabilized bias to the InGaAs photo-diode. The controlled CTIA current drives the pixels to achieve the required response and speed. Figure 6 shows the measured temporal response of the *Cardinal* detectors to a short pulse. In the first generation design implemented in *Cardinal-640* we find a response time constant of 6µs. In the second generation design introduced in the *Cardinal-640-LN* and in the *Cardinal-1280* the time constant decreases to a sub-1µs without compromising the integration efficiency. The edges of the response in both *Cardinal-640-LN* and *Cardinal-1280* are sharp, revealing rapid gating capabilities without smearing the temporal response of the pulse, e.g. for a 100ns pulse the gate corresponds to a theoretical 15m depth resolution.

Figure 7 (left) shows an image taken with the *Cardinal- 640-LN* in Gated mode. The target image is illuminated by a 50ns laser pulse at a wavelength of 1.5µm, synchronized to the camera, and the integration time is set to 1µs. For a comparison we also show (right) the image taken with an ambient light along with the laser, with a 4ms integration time. The laser illumination is the bright spot on the target.

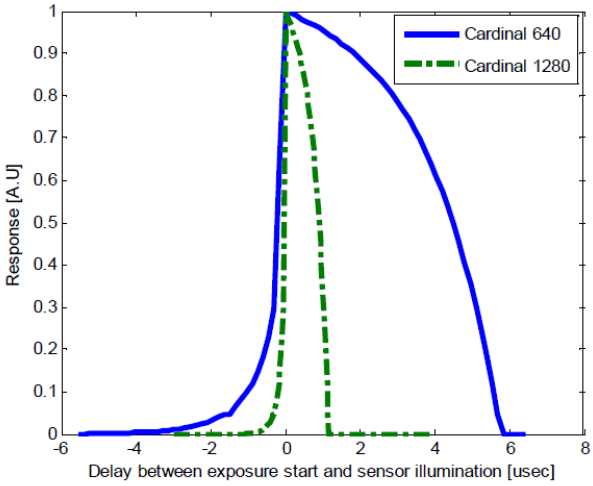

Figure 6: Photo-induced CTIA response to 30ns, 1.55µm laser pulse incident on the sensor at different delay time with regard to the integration window rising at t=0

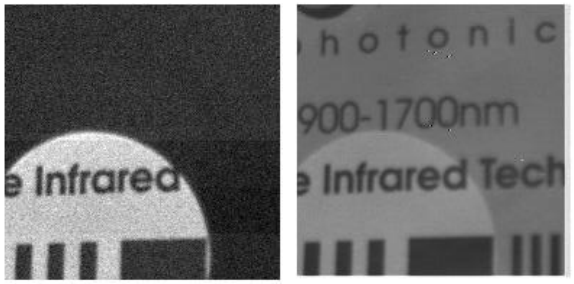

Figure 7: Gated imaging in *Cardinal-640-LN* with 1µs integration time while illuminated by a 1.55µm laser pulse (left). The same image with additional ambient light at 4ms integration time (right)

4. LASER PULSE DETECTION

A unique feature available in both *Cardinal-640* and *Cardinal-1280* sensors is the possibility to detect very efficiently short laser pulses and present their position on the image frame, thus negating the need to calibrate the field of view of additional camera as well as provide a fast laser detection. For each pixel in these FPAs, a designated bit in the output video indicates whether a pulse was detected between imaging readouts. The Laser Pulse Detection (LPD) circuit is seeking fast signal variation in real-time, where an event is detected by measuring a positive current change indicative of an increased radiance change during each frame. The fast change is detected by measuring the derivative of the current after passing through a band-pass filter, which is designed to remove the DC component of the photodiode input signal current. Accordingly, the AC component is detected with increased sensitivity.

The fast event detection is carried out simultaneously and in parallel to the standard integration imaging.

Figure 8 compares three generations of LPD design in SCD's InGaAs sensors. The LPD duty cycle of *Cardinal-640* decreases rapidly with increasing frame rate reaching below 1% duty cycle at the highest frame-rate of 330Hz, whereas the *Cardinal-1280* Detection While Read (DWR) mode shows a decrease to about 82% duty cycle at 350Hz. The *Cardinal-1280* Detection-only mode shows only a minor decrease to 95% at 350Hz. A 3rd generation LPD circuit was implemented in the new InGaAs *SWIFT* sensor, where the novel design will provide nearly 100% duty-cycle at an exceptional 50kHz frame-rate.

The LPD mode of these sensors can be operated at the system level either Synchronously (SLPD) or Asynchronously (ALPD) with a pulsed laser. Figures 9 and 10 demonstrate the ALPD function in *Cardinal-1280*.

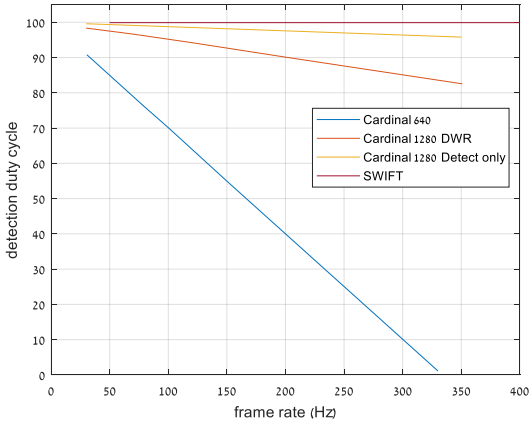

Figure 8: Laser pulse detection duty-cycle in percentage versus imaging frame-rate in the *Cardinal* sensors. *SWIFT* is a new sensor showing an almost 100% LPD duty-cycle at frame-rates of up to 50 kHz

Figure 9: Demonstration of the ALPD mode in *Cardinal-1280*. The white spot on the target presents the additional LPD bit in the pixels where a laser pulse was detected. Part of the laser path from right to the target was also detected and is seen on the image as dotted white line

Figure 10: Similar to Figure 9, at a different scenery, the laser pulse from above was detected on the silo

Figure 11 depicts the estimated range of laser pulse detection in a typical system that uses the LPD mode of *Cardinal-1280*. Table 1 holds the main parameters used in this calculation. We find that 7km detection range is expected for a 2mJ laser pulse intensity, while almost 17km range is achievable for 27mJ pulse.

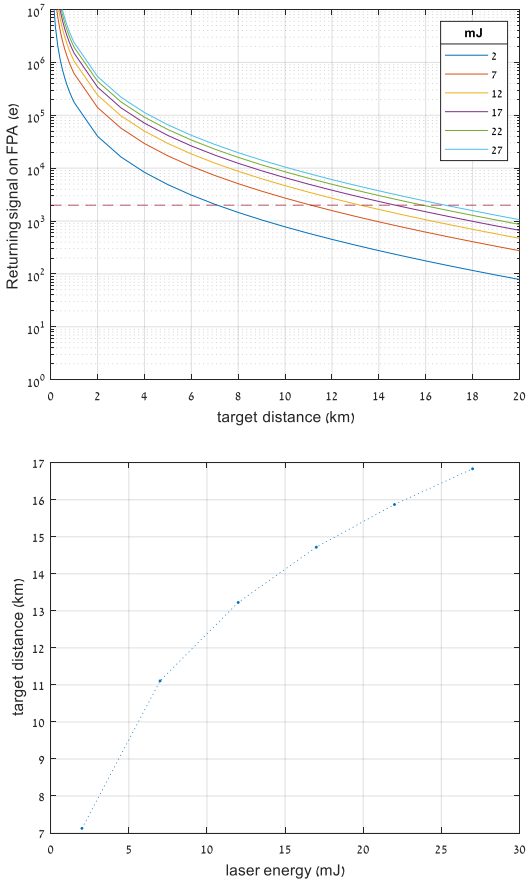

Figure 11: *top*: The calculated returning laser signal in *Cardinal-1280* (in e^-) for various pulsed laser energies (solid lines). The threshold level set to $2ke^-$ is the dash line. *Bottom*: The maximum detectable target distance

Table 1: Laser range calculation parameters

Parameter	Value
Focal length	100mm
F/#	4
Target reflectance	75% (aluminium metal roof) [7]
Laser divergence	80% of the energy at 0.5mrad
Laser wavelength	1.54µm
Optical transmission	90%
Atmospheric transmission	Mid-latitude urban model

5. SUMMARY

In this work we presented SCD's *Cardinal* sensors for the SWIR spectral band. The InGaAs based FPAs use CTIA stage for LNIM (LLL conditions), with full-well capacity of 12÷15ke$^-$ and low readout noise. For standard imaging (SIM) at high flux the full-well capacity is 0.3÷1.0Me$^-$. Gated imaging in *Cardinal-640-LN* and *Cardinal-1280* is used over selectable Region of Interests (ROI) with fast integration. Sensitive in-pixel laser pulse detection capability is implemented in the *Cardinal-640*, *Cardinal-1280,* and *SWIFT* sensors. The pulse detection can be either synchronous or asynchronous to the illuminating laser with a sensitivity of 500e$^-$ / pixel.
Table 2 summarizes the main features and performance of the *Cardinal* family of detectors.

Table 2: *Cardinal* detector family main performance

Parameter	Cardinal 640	Cardinal 640 LN	Cardinal 1280
Format	640×512		1280×1024
Pitch	15 µm		10 µm
QE	> 70%		
Dark Current (20°C)	5 fA	1.5 fA	1.25 fA
LNIM well capacity	15 ke$^-$	13 ke$^-$	12 ke$^-$
LNIM Readout noise	40 e$^-$	15 e$^-$	35 e$^-$
LNIM NEP	0.3 fW	0.13 fW	0.16 fW
Frame rate (LNIM CDS)	160 Hz		
SIM well capacity	0.3 Me$^-$	0.5 Me$^-$	0.5, 1 Me$^-$
SIM Readout noise	150 e$^-$	210 e$^-$	170e$^-$, 350 e$^-$
Gate width	6 µs	0.5 µs	1 µs
Frame rate (SIM)	350 Hz		
Special Modes	TLRF ALPD	HDR	ALPD

6. REFERNCES

1. Espinola, R., Jacobs, E., Halford, C., Vollmerhausen, R., Tofsted, D., Vol. 15, No.7, OPTICS EXPRESS 3816, April 2007
2. Leinert, Ch., Bowyer, S., Haikala, L.K., Hanner, M.S., Hauser, M.G., Levasseur-Regourd, A.-Ch., Mann, I., Mattila, K., Reach, W.T., Schlosser, W., Staude, H.J., Toller, G.N., Weiland, J.L., Weinberg, J.L., Witt, A.N., Astron. Astrophys. Suppl. Ser. 127, 1-99 (1998)
3. R. Fraenkel, E. Berkowicz, L. Bykov, R. Dobromislin, R. Elishkov, A. Giladi, I. Grimberg, I. Hirsh, E. Ilan, C. Jacobson, I. Kogan, P. Kondrashov, I. Nevo, I. Pivnik, S. Vasserman, Proc. SPIE 9819, 981903 (2016)
4. O. Ofer, R. Elishkov, R. Friedman, I. Hirsh, L. Langof, M. Nitzani, Y. Reem, C. Jakobson, I. Pivnik, E. Louzon, R. Fraenkel, B. Milgrom, I. Shtrichman, SPIE 11741, 1174108 (2021)
5. I. Hirsh, E. Louzon, A. Aharon, R. Gazit, D. Bar, P. Kondrashov, M. Weinstein, M. Savchenko, M. Regensburger, A. Navon, E. Shunam, O. Rahat, A. Mediouni, E. Mor, A. Shay, R. Iosevich, M. Ben-Ezra, A. Tuito, I. Shtrichman, Proc. SPIE 10624, 1062406 (2018)
6. Chih-Cheng Hsieh, Chung-Yu Wu, Far-Wen Jih and Tai-Ping Sun, IEEE Transactions on Circuits and Systems for Video Technology, vol. 7, no. 4, 594, (1997)
7. A.M. Baldridge, S.J. Hook, C.I. Grove, Rivera G., Remote Sensing of Environment 113(4), 711 (2009)